Final Report

Title: Structural health monitoring pertaining to critical aircraft structural components

AFOSR/AOARD Reference Number: AOARD-08-4051

AFOSR/AOARD Program Manager: Dr Kumar Jata.

Period of Performance: 27 September 2008 – 27 September 2009

Submission Date: March 2010

PI: W.K. Chiu, Monash University

Report Documentation Page

Form Approved
OMB No. 0704-0188

1. REPORT DATE	2. REPORT TYPE	3. DATES COVERED
19 MAR 2010	**Final**	**15-09-2008 to 15-03-2010**

4. TITLE AND SUBTITLE	5a. CONTRACT NUMBER
Structural health monitoring pertaining to critical aircraft structural components	**FA23860814051**
	5b. GRANT NUMBER
	5c. PROGRAM ELEMENT NUMBER
6. AUTHOR(S)	5d. PROJECT NUMBER
Wing Kong Chiu	5e. TASK NUMBER
	5f. WORK UNIT NUMBER
7. PERFORMING ORGANIZATION NAME(S) AND ADDRESS(ES)	8. PERFORMING ORGANIZATION REPORT NUMBER
Monash University,P.O. Box 31,Monash University, Wellington Road,Clayton, Victoria ,AU,3800	**N/A**
9. SPONSORING/MONITORING AGENCY NAME(S) AND ADDRESS(ES)	10. SPONSOR/MONITOR'S ACRONYM(S)
Asian Office of Aerospace Research & Development, (AOARD), Unit 45002, APO, AP, 96338-5002	**AOARD**
	11. SPONSOR/MONITOR'S REPORT NUMBER(S)
	AOARD-084051

12. DISTRIBUTION/AVAILABILITY STATEMENT

Approved for public release; distribution unlimited

13. SUPPLEMENTARY NOTES

14. ABSTRACT

The aim of this project was to develop and validate efficient computational and experimental tools for characterizing the temporal and spatial features of incident stress wave necessary for the efficient generation of a circumferential creeping wave and its associated reradiated bulk wave in open holes using low profile surface mounted actuators and exploit the circumferential creep wave and its associated reradiated bulk wave for the detection and monitoring of service induced defects in hard-to-inspect regions.

15. SUBJECT TERMS

Aircraft Structures, Aging Aircraft, Non-destructive Evaluation

16. SECURITY CLASSIFICATION OF:			17. LIMITATION OF ABSTRACT	18. NUMBER OF PAGES	19a. NAME OF RESPONSIBLE PERSON
a. REPORT	b. ABSTRACT	c. THIS PAGE			
unclassified	**unclassified**	**unclassified**	**Same as Report (SAR)**	**12**	

Objectives: The objectives of this project are to

(1) develop and validate efficient computational and experimental tools for characterising the temporal and spatial features of incident stress wave necessary for the efficient generation of a circumferential creeping wave and its associated reradiated bulk wave in open holes using low profile surface mounted actuators.

(2) Exploiting the circumferential creep wave and its associated reradiated bulk wave for the detection and monitoring of service induced defects in hard-to-inspect regions.

Status of effort: Below describes a major component of the work performed.

1. Specimen Geometry and Lamb Wave Generation

An aluminium I-beam with dimensions 101.6 x 76.2 x 4.75 / 6.35 mm was cut into 300 mm sections. A flange was removed such that the section took T-form (figure 1). A 10 mm diameter through-hole was fabricated with the centre located 20 mm from the bottom surface of the flange. Lamb waves were generated in the riser with surface bonded piezoelectric discs. Hence, the piezoelectric actuator was bonded with a two-part epoxy adhesive 26 mm from the hole centre to have a line of sight of a 3 mm notch in the riser. The notch was cut with a 0.5 mm wide blade in 1 mm increments to a length of 3 mm (figure 2). The spatial wavelengths of the propagating waves were of similar dimension to the hole in the riser using an appropriate excitation frequency. A 10mm diameter, 1mm thick, Ferroperm Pz26 ceramic disc was chosen for Lamb wave generation. The idealised fundamental planar resonant frequency of this particular disc is 220 kHz, corresponding to a spatial wavelength of 11 mm for the propagating A_0 Lamb mode in a 4.75 mm thick aluminium plate. Taking advantage of the resonant behaviour of the low-profile piezoceramic actuator enables not only for good signal-to-noise response from laser vibrometry, but for the A_0 mode to be propagated in the incident wave. In this configuration, figure 3 shows that the A_0 Lamb mode is essentially non-dispersive above 200 kHz. The dispersive effect, which can cause significant attenuation of particularly the A_0 Lamb mode, can be further minimised by using a narrow bandwidth windowed tone burst rather than a wideband pulse for actuation. A compromise must then be made with respect to the signal length and number of cycles of the tone burst. A four cycle Hanning windowed sinusoidal tone burst was chosen such that the incident packet propagating around the hole can be isolated from the waves reflecting from the top edge of the riser.

2. Automated Laser Vibrometry

A computer controlled laser vibrometry rig pictured in figure 4 was developed at Monash University for use in this experiment. A Parker Automation 404XE Electromechanical Positioning System with LV233 stepper motors was used to position the specimen with custom software developed in MATLAB. The software was developed to synchronise positioning with signal generation and data acquisition. The stepper motors, capable of a resolution of 5000 steps per millimetre, enabled extremely accurate and consistent positioning of the specimen.

Lamb wave responses of the plate were sensed using a three axis laser vibrometer. A Polytec CLV 3D sensor head with left, right and top beams, was positioned and focussed to measure three components of velocity (V_L, V_R and V_T) of the specimen at any given position. The 1.5 MHz modified CLV-M030.B decoder module outputs a voltage which is directly proportional to the velocity with a factor of 25 mm/s/V. The signals were further low-pass filtered and amplified by 20 dB through a Krohn-Hite Model 3944 Programmable 4-Channel 2 MHz Filter. The velocity signals were later converted in MATLAB to their orthogonal components, knowing the 12 degree angle between the optical axis and the top laser beam with the 160 mm focal length lens, using the supplied equations.

Data acquisition was performed with a National Instruments PCI-6115 board and BNC-2110 block at 10 MHz and passed to the controlling computer for storage. Input capture from the laser was hardware triggered by the rising edge of the PZT excitation signal. This was essential for ensemble averaging and synchronisation of spatially varying data. In this case, 16 velocity-time series averages were performed at each scan location to enhance the signal-to-noise ratio for a series length of 1 millisecond. The excitation signals were amplified from the 10 V output at 4 MHz by 14 dB with a Krohn-Hite Model 7602 Wideband Power Amplifier.

3. Experimental Results and Discussion

3.1. Visualisation and Comparison of Circumferential Creeping Wave Generation by A_0 Lamb Modes

In defining the weep hole centre as the origin of the scanned grid, the in-plane velocity field can be converted to cylindrical co-ordinates using the following transformations, with V_r as the radial component of velocity and V_θ as the azimuthal component of velocity:

$$V_r = V_x \cos\theta + V_y \sin\theta \quad , \quad V_\theta = -V_x \sin\theta + V_y \cos\theta \, , \tag{3}$$

The scattering of the velocity field from the inclusion of damage can then be visualised by a subtraction of the damaged velocity field from the defect free baseline velocity field:

$$V_{scatter}(t) = V_{baseline}(t) - V_{damage}(t) \quad (4)$$

Nagy et al. [1] asserted that peripheral rays within one wavelength of a vertically polarized shear (SV) wave are well coupled to the leaky Rayleigh wave creeping around a hole. Like SV waves, Lamb waves are vertically polarised. The fundamental A_0 has significant a shear component whereas the S_0 does not.

With the 220 kHz excitation, the two dimensional fast Fourier transform (2D FFT) along a vertical line above the actuator (figure 2) shows that the A_0 Lamb mode in the incident wave is roughly 65% the amplitude of the S_0 Lamb mode (figure 5). With a hole radius of 5 mm and a shear velocity of 3103 m/s for aluminium, [2] suggests that for 220 kHz, the creeping wave group velocity should be only 10% less than that of the propagating A_0 mode. This is supported using the V_z field of figure 6 and the slight hook in the wavefront of the propagating A_0 wave attached to the free surface of the hole. The notch causes significant interference to wave propagation of the 220 kHz signal by collecting and concentrating the wave energy. The creeping wave generated on the leading side of the hole ascends the leading face of the notch, wraps around the tip and descends the trailing face of the notch to continue to propagate as a creeping wave on the trailing side of the weep hole. As the creeping wave propagates along the trailing face of the weep hole, it is seen to shed energy into the riser.

The transformation to a cylindrical co-ordinate system is beneficial in isolating the radial specular reflections and shed waves from the azimuthal spiralling circumferential creeping waves caused by the presence of the notch (figure 7). The scattered velocity field, with the S_0 Lamb mode being approximately 65% the amplitude of the A_0 Lamb mode (figure 8), maintains its form and grows in amplitude as the notch length in increased. This signature behaviour is potentially the key for non-destructive evaluation (NDE) of the structure.

3.2. Exterior Quantitative Evaluation

Having shown that the presence of the notch causes significant scattering to the incident wave on the riser, the next step is to ascertain that this scattering is detectable from outside the fuel tank. To do this, a line scan on the flange is used to show the variation of surface velocity with time and distance from the weep hole. An optimised position to locate a piezoelectric receiver was then chosen for further evaluation using the results of the line scan.

The directions for the components of velocity in-plane V_{xf} (T beam axis) and out-of-plane V_{zf} are shown in (figure 2) with the origin being directly below the centre of the weep hole. With the 220 kHz input (figure 9), the scattered V_{zf} field reveals the addition of a Hanning windowed sinusoidal pulse from the notch, sweeping along the flange (figure 10). This scattered pulse peaks in amplitude approximately 50 mm from the weep hole centre. The time series for V_{zf} extracted at 50 mm (figure 11) shows a growth in amplitude as the notch length is increased. The reverse happens for V_{xf} at this position, with a reduction in amplitude as the notch length is increased, but to a lesser extent. The scattered pulse responsible for the change in amplitudes spans 35-70 μs (figure 12). This leads to the expectation that the dominant increased difference in V_{zf} over decreased V_{xf} will cause an increased PZT voltage output for damage should one be bonded to the flange at this location. To demonstrate this, a 5 mm diameter, 1 mm thick, Ferroperm Pz27 ceramic disc was bonded to the flange 50 mm from the weep hole centre. The voltage – time response of the PZT is shown in figure 13. A similar trend occurs to that of the V_{zf} response, with an increase in signal amplitude from the arrival of the additional pulse from the damage. Taking a FFT of the Hanning windowed scattered voltage (35-70 μs) shows the potential of this technique to detect damage with a clear increase in amplitude for damage at the 220 kHz excitation frequency.

Concluding Remarks

The above findings are important to for the in-situ structural health monitoring of hard-to-inspect regions on an aircraft structure. This work shows how the generation of a secondary wave mode can be scattered by sub-surface defects. The exploitation of this secondary wave field can be extended for the stress wave based structural health monitoring methodology.

References:

1. Nagy, P.B., M. Blodgett, and M. Golis, *Weep Hole Inspection by Circumferential Creeping Waves.* NDT & E International, 1994. **27**(3): p. 131-142.
2. Hassan, W. and P.B. Nagy, *Circumferential Creeping Waves around a Fluid-Filled Cylindrical Cavity in an Elastic Medium.* The Journal of the Acoustical Society of America, 1997. **101**(5): p. 2496-2503.

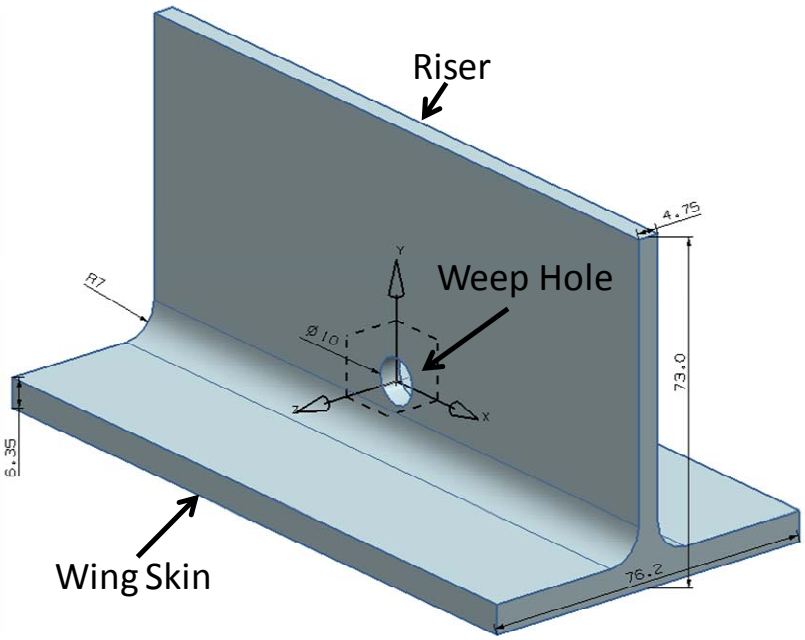

Figure 1. Dimensioned model of the riser with co-ordinate axes.

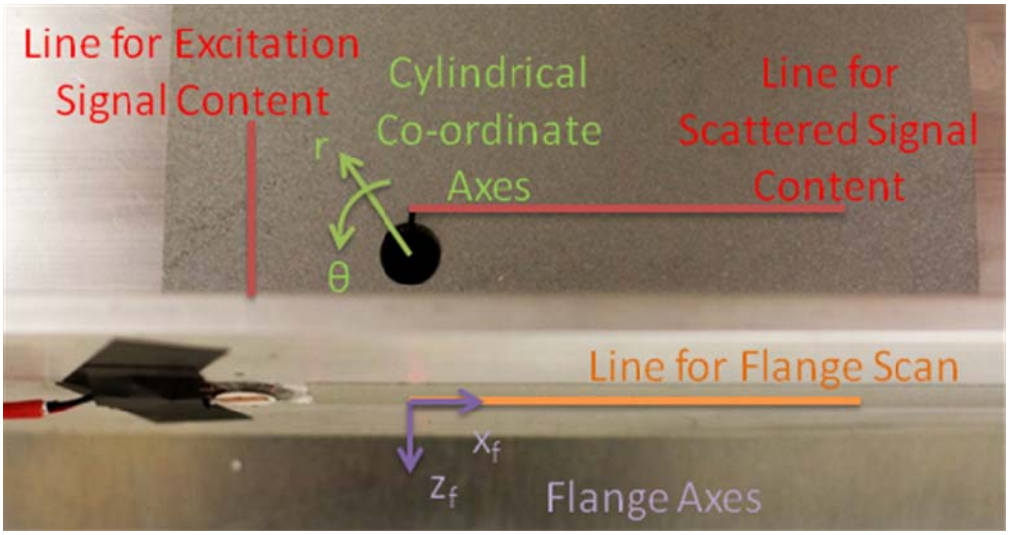

Figure 2. Photograph of test specimen showing the relative positioning of a PZT actuator to a weep hole with simulated fatigue damage.

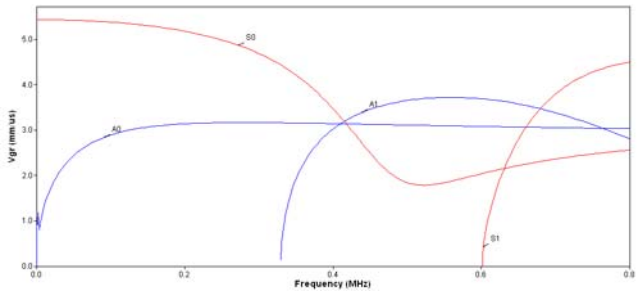

Figure 3. Plot of group velocity against frequency for the A_0, S_0 and A_1 Lamb modes in a 4.75 mm thick aluminium plate.

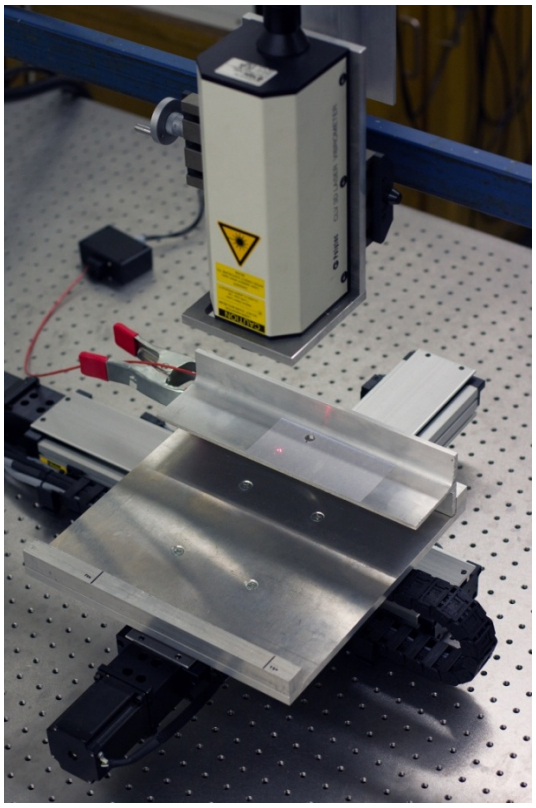

Figure 4. The laser vibrometry rig developed at Monash University for scanning the test specimen.

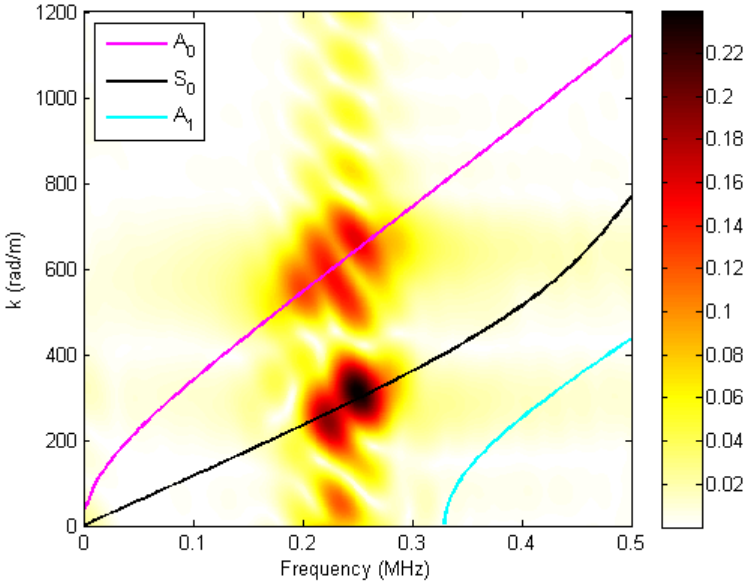

Figure 5. Content of the 220 kHz excitation signal.

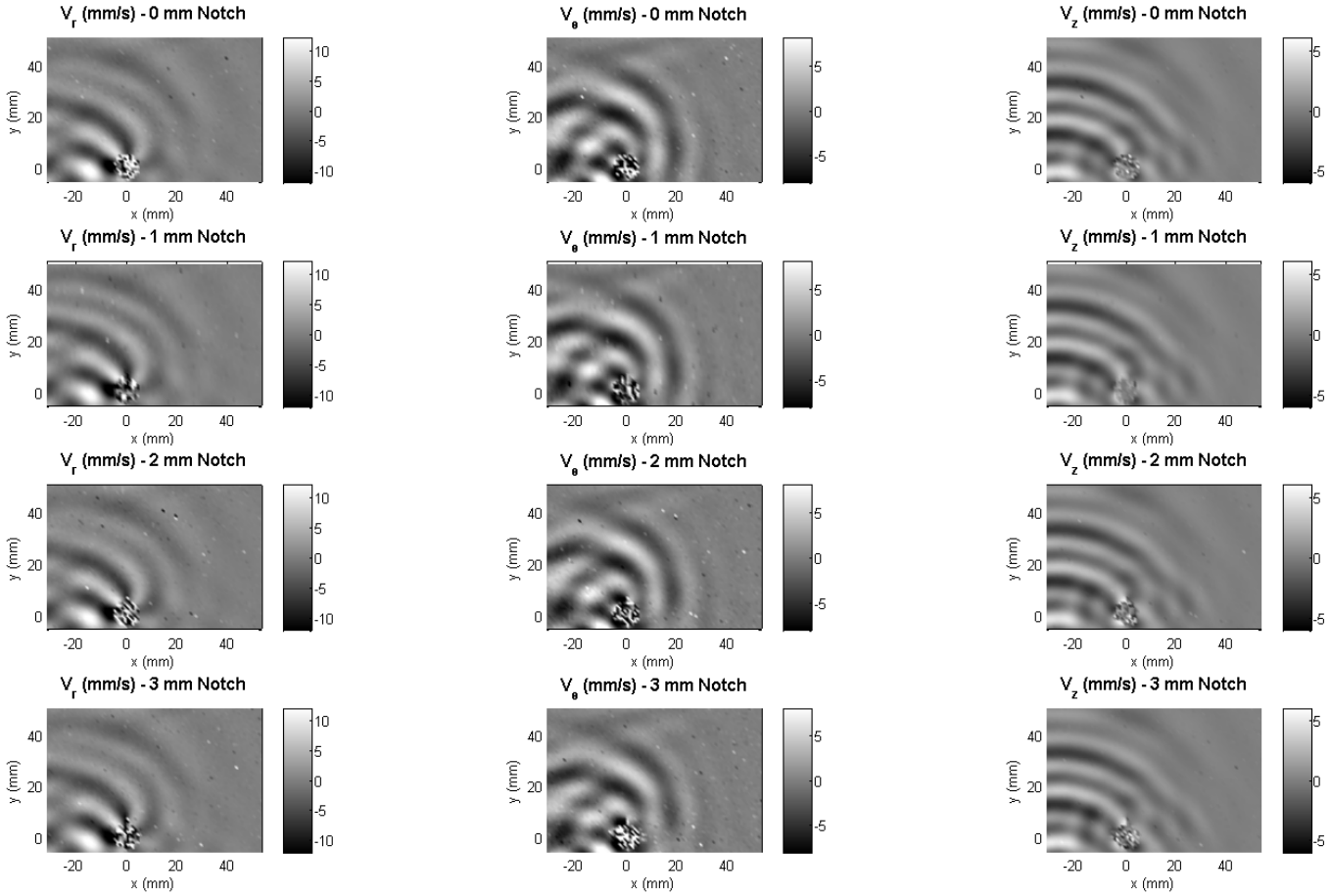

Figure 6. Cylindrical velocity field of the 220 kHz signal on the riser at 35 microseconds. The left, centre and right columns display the radial, azimuthal and out-of-plane components of velocity respectively.

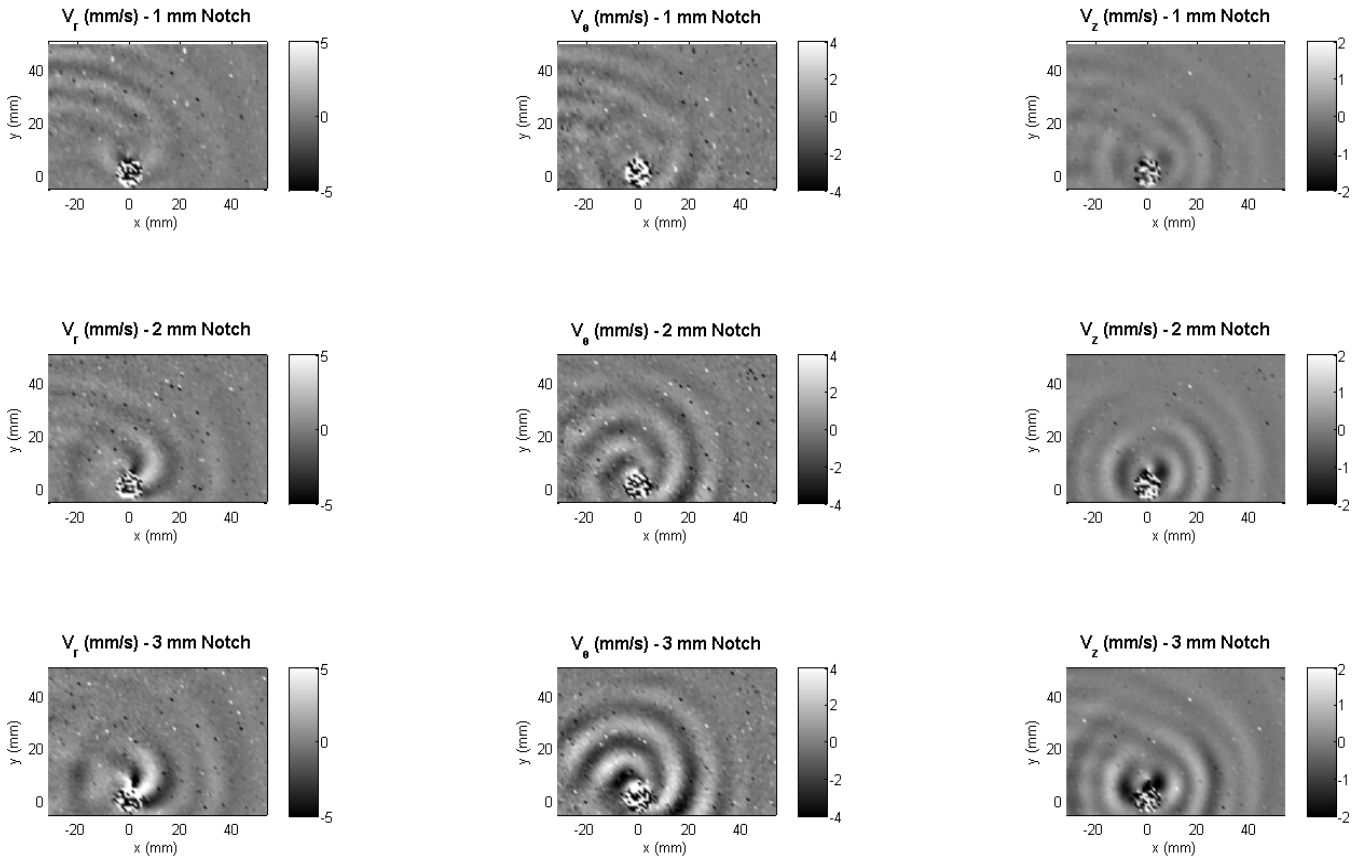

Figure 7. Cylindrical scattered velocity field of the 220 kHz signal on the riser at 35μs. The left, centre and right columns display the radial, azimuthal and out-of-plane components of velocity respectively.

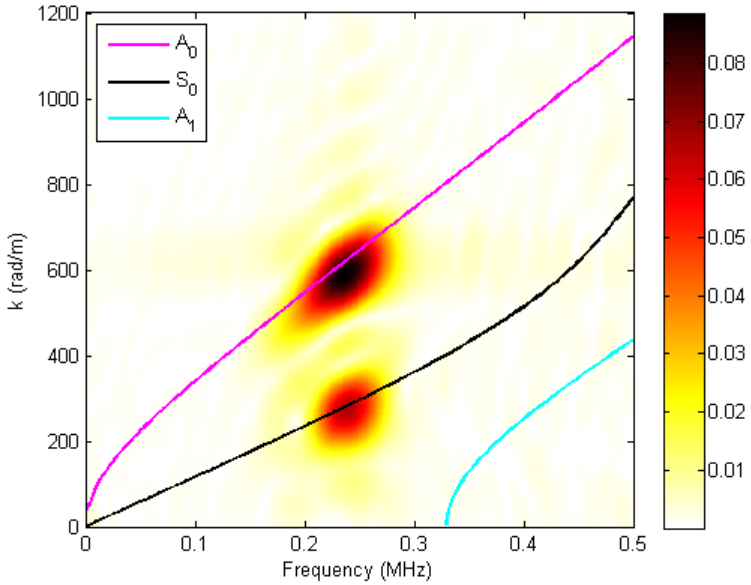

Figure 8. Content of the 220 kHz scatter from the notch.

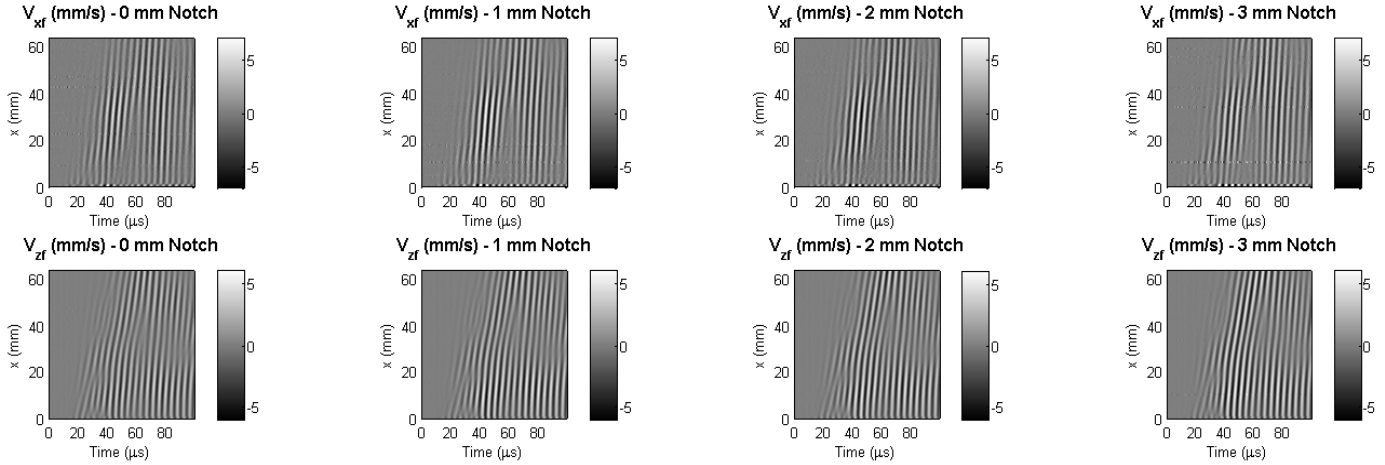

Figure 9. Velocity field from the 220 kHz signal along the flange.

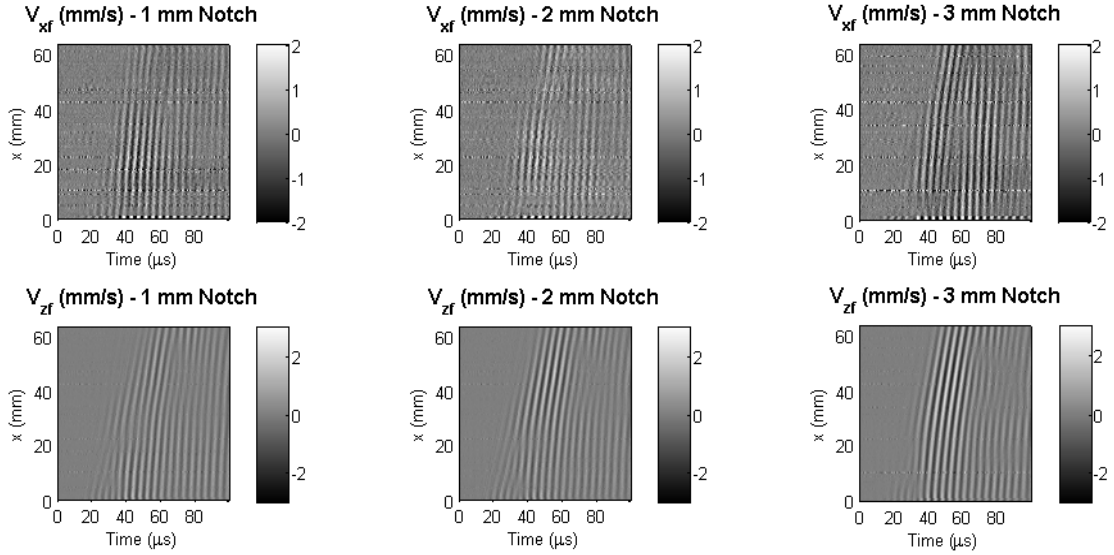

Figure 10. Velocity scatter from the 220 kHz signal along the flange.

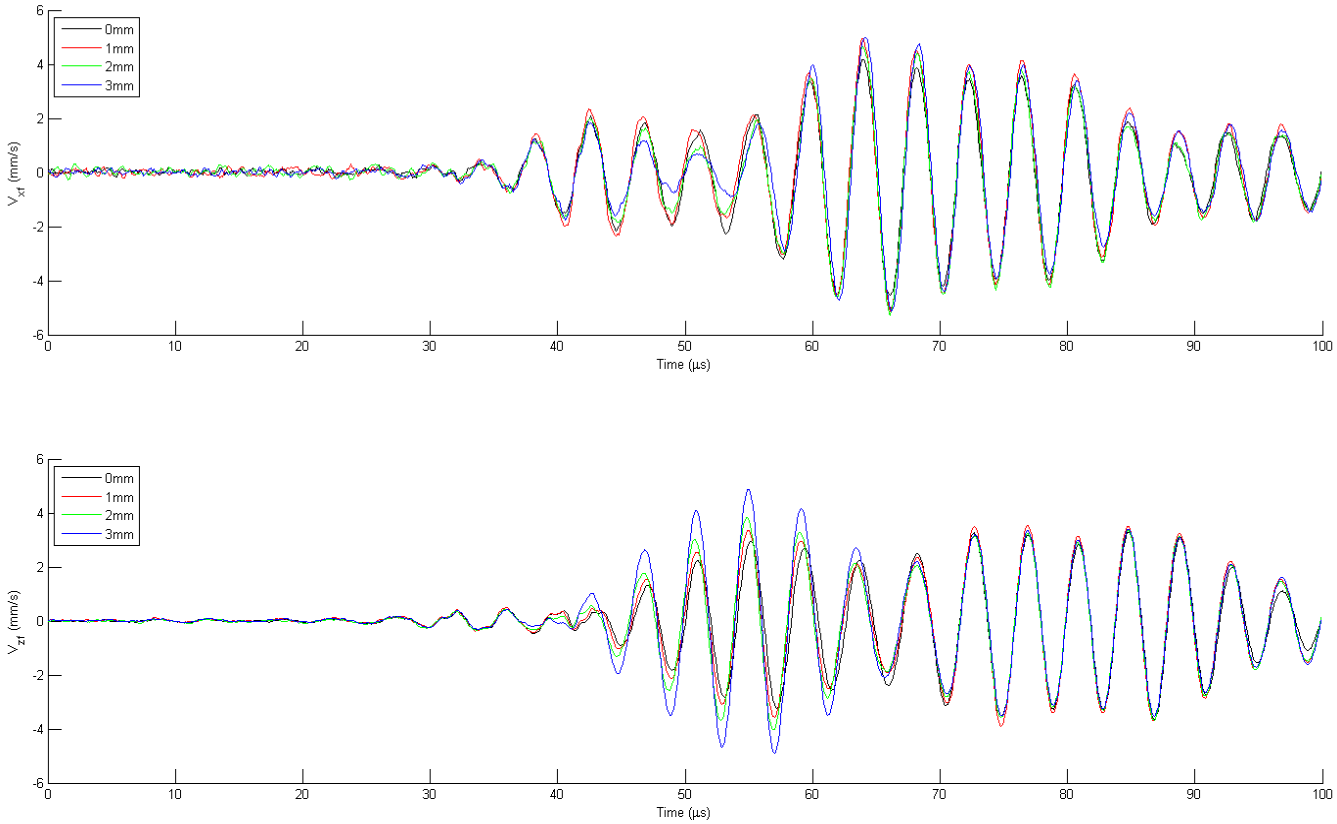

Figure 11. Time series extracted from figure 15 at 50 mm for V_{xf} and V_{zf}.

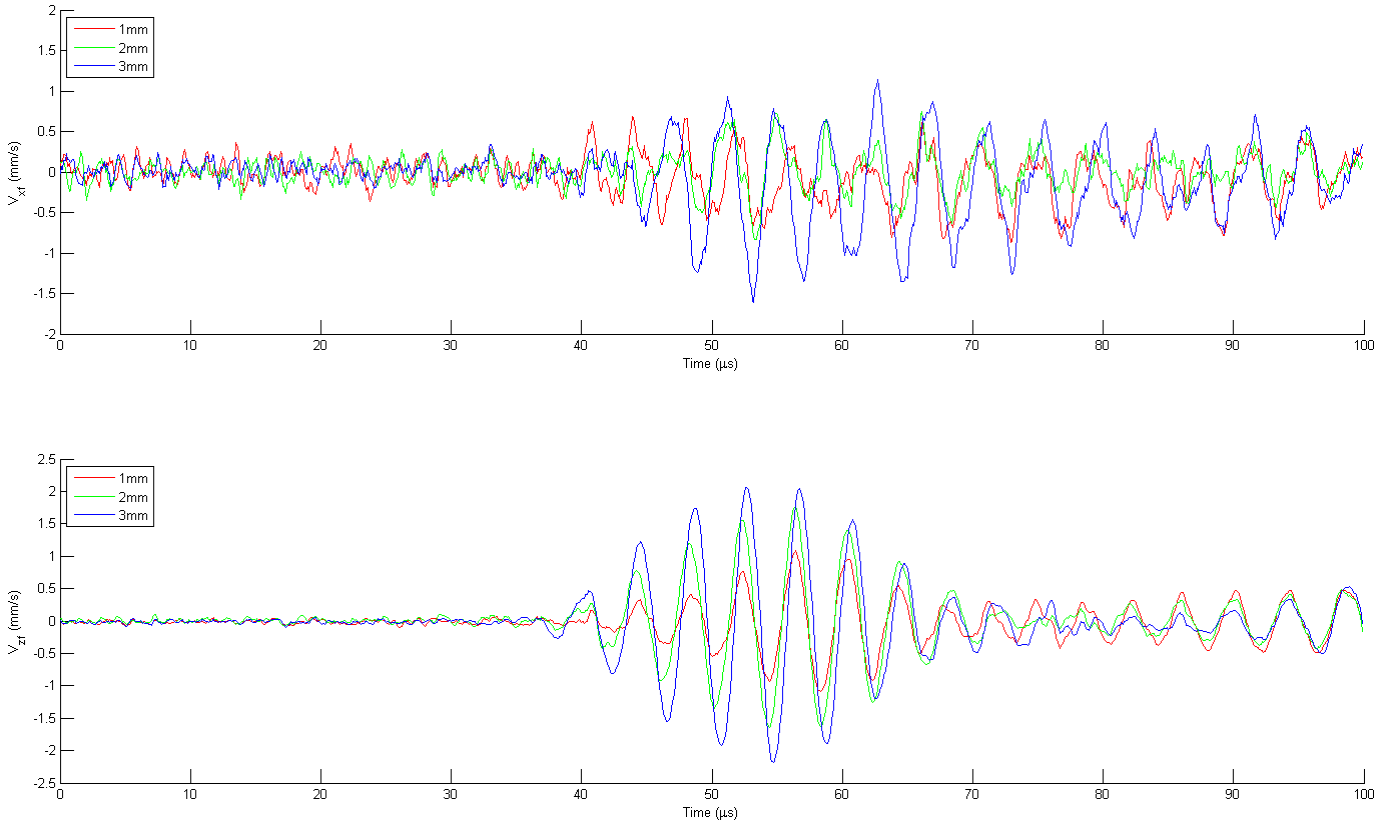

Figure 12. Scatter time series formed from Figure 16 at 50 mm for V_{xf} and V_{zf}.

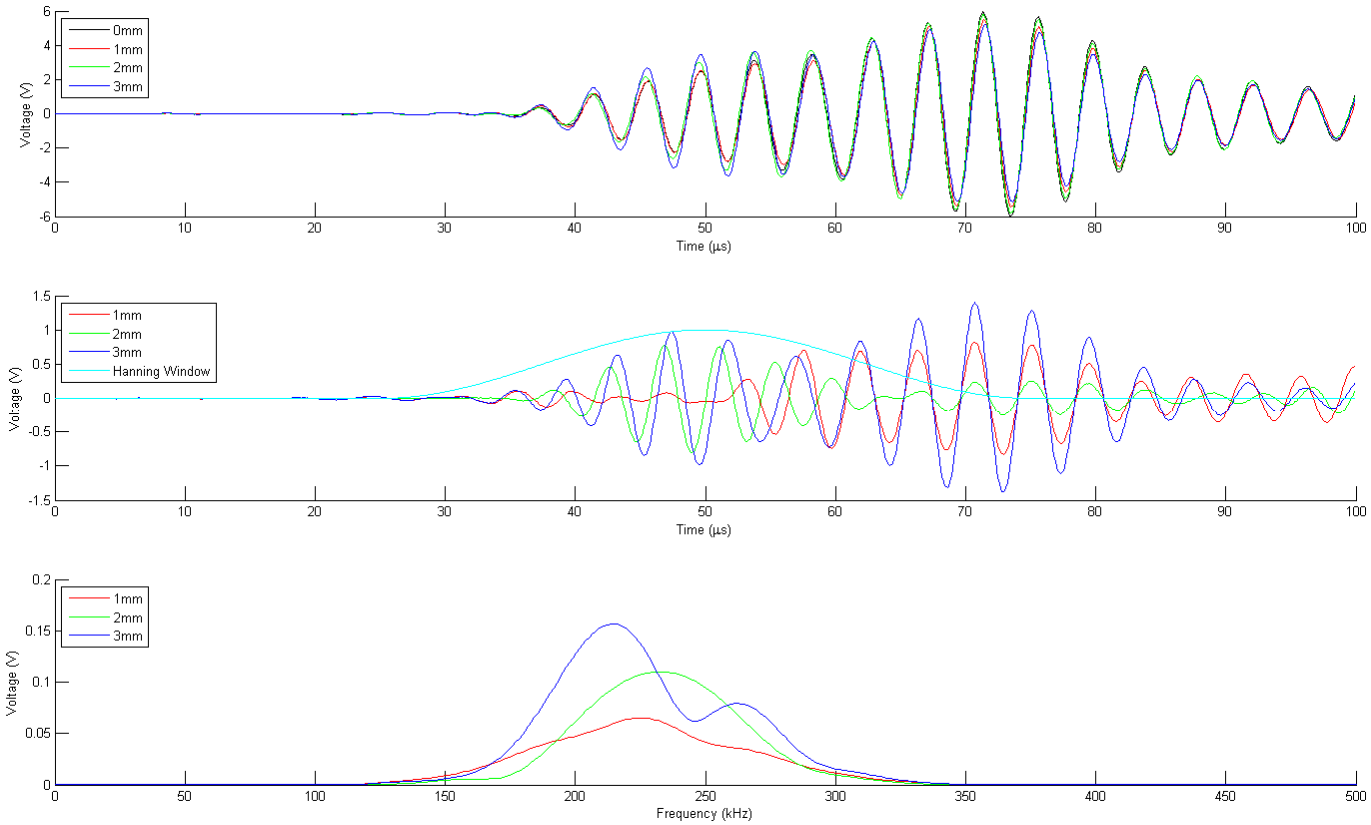

Figure 13. Voltage acquired from a PZT bonded on the flange, 50 mm from the weep hole centre for the 220 kHz signal.

Abstract: This project deals with the investigation into the viability of using acousto-ultrasonic methodology for the in-situ structural health monitoring of the development of top-cracks in fuel weep holes in the USAF A-10 aircraft. One of the significant findings of this project is the recent experimental evidence confirming that circumferential creeping waves can be produced in a weep hole using surface mounted piezoelectric elements. Some experiments demonstrated the ability to monitor the development of an upward developing fine saw cut simulating the upward developing fatigue crack in the riser of the A10 aircraft. These results clearly highlighted the scattering of the circumferential creeping wave and the reradiated bulk wave by this upward growing crack. It also highlighted the potential in incorporating this phenomenon for in-situ SHM. Our current work has generated a plethora of research questions that when answered will propel this type of SHM to the next level. Some of the future work that is required include;

#1: Understanding the essential temporal and spatial characteristics of the incident stress wave to efficiently generate the circumferential creeping wave and the reradiated bulk wave in the weep hole

#2: Understanding how the circumferential creeping wave generated at the open hole in the riser manifests itself on the surface of the wing panel through geometry change in the vicinity of the T-section at the intersection between the riser and the wing skin.

#3: If this circumferential creeping wave can be monitored on the surface of the wing panel, what physics is involved in relating the defect size to the characteristics of this creeping wave mode?

Personnel Supported: A PhD student (Cain Doherty) is supported with this proposal

Publications: We are currently preparing 1 paper for Structural Health Monitoring – an International Journal; and 1 conference paper for the Australasian Congress on Applied Mechanics (Perth, Dec 2010), 1 paper for the Asia-Pacific Workshop on Structural Health Monitoring (Tokyo, Nov 2010).

Interactions: Participation in International Workshop on Structural Health Monitoring (Sep 2009).

Inventions:

None

Honors/Awards: None

Archival Documentation: The papers, when submitted will be copied onto Dr Kumar Jata.

Software and/or Hardware (if they are specified in the contract as part of final deliverables): None